AFCRL-68-0522

ANALYSIS OF LIDAR DATA OBTAINED UNDER CONDITIONS OF LOW CEILING AND VISIBILITY

WILLIAM VIEZEE EDWARD E. UTHE

STANFORD RESEARCH INSTITUTE
333 RAVENSWOOD AVENUE
MENLO PARK, CALIFORNIA 94025

CONTRACT NO. F 19628-68-C-0021
PROJECT NO. 6670
TASK NO. 667002
WORK UNIT NO. 66700201

Scientific Report No. 1

August 1968

Contract Monitor: WILBUR H. PAULSEN
Aerospace Instrumentation Laboratory

Prepared for

AIR FORCE CAMBRIDGE RESEARCH LABORATORIES
OFFICE OF AEROSPACE RESEARCH
UNITED STATES AIR FORCE
BEDFORD, MASSACHUSETTS 01730

STANFORD RESEARCH INSTITUTE
MENLO PARK, CALIFORNIA

40

DISCLAIMER NOTICE

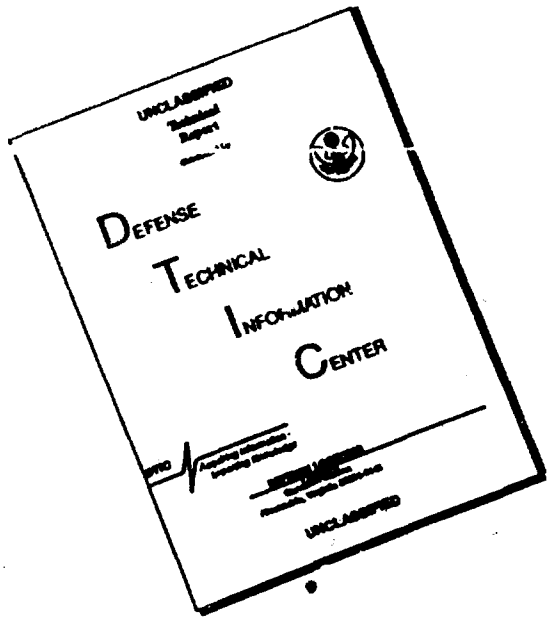

THIS DOCUMENT IS BEST QUALITY AVAILABLE. THE COPY FURNISHED TO DTIC CONTAINED A SIGNIFICANT NUMBER OF PAGES WHICH DO NOT REPRODUCE LEGIBLY.

AFCRL-68-0522

ANALYSIS OF LIDAR DATA OBTAINED UNDER CONDITIONS OF LOW CEILING AND VISIBILITY

WILLIAM VIEZEE EDWARD E. UTHE

STANFORD RESEARCH INSTITUTE
333 RAVENSWOOD AVENUE
MENLO PARK, CALIFORNIA 94025

CONTRACT NO. F 19628-68-C-0021
PROJECT NO. 6670
TASK NO. 667002
WORK UNIT NO. 66700201

Scientific Report No. 1

August 1968

Contract Monitor: WILBUR H. PAULSEN
Aerospace Instrumentation Laboratory

Prepared for

AIR FORCE CAMBRIDGE RESEARCH LABORATORIES
OFFICE OF AEROSPACE RESEARCH
UNITED STATES AIR FORCE
BEDFORD, MASSACHUSETTS 01730

ABSTRACT

Lidar (laser radar) data obtained at Hamilton AFB, California, under conditions of low ceiling and visibility are analyzed by hand and by electronic computer to explore the operational utility of lidar in determining cloud ceiling and visibility for aircraft landing operations. Hand analyses of the data show the ability of the lidar to describe the spatial configuration of the low-cloud structure along the landing-approach path. The problems inherent in evaluating lidar observations are discussed, and initial approaches to quantitative solutions by computer are presented. It is demonstrated that operationally useful information on the ceiling and visibility conditions contained in the hand analyses can be presented by digitizing the lidar data and subjecting these data to computer analysis.

LIST OF CONTRIBUTORS

The following personnel from Stanford Research Institue contributed to the research reported on in this document:

Ronald T. H. Collis, Director, Aerophysics Laboratory, Project Supervisor

William Viezee, Research Meteorologist, Project Leader

Edward E. Uthe, Atmospheric Physicist

H. Shigeishi, Mathematician

R. Trudeau, Meteorological Assistant

N. B. Nielson, Senior Electronics Technician

W. D. Dyer, Electromechanics Technician

CONTENTS

ILLUSTRATIONS

TABLES

I INTRODUCTION

On 8 and 9 January 1968, the SRI Mark V pulsed ruby lidar was activated at Hamilton AFB, California, in order to explore the operational utility of the lidar in cloud ceiling and visibility determination for aircraft landing operations. Because of a unique location of the airfield on the western edge of San Pablo Bay (see Fig. 1), the aircraft landing operations are confronted with a difficult meteorological problem. San Pablo Bay with its relatively cold water is a notorious source of fog and low stratus, particularly in winter. The landing-approach glide path begins over the marshes and open water of

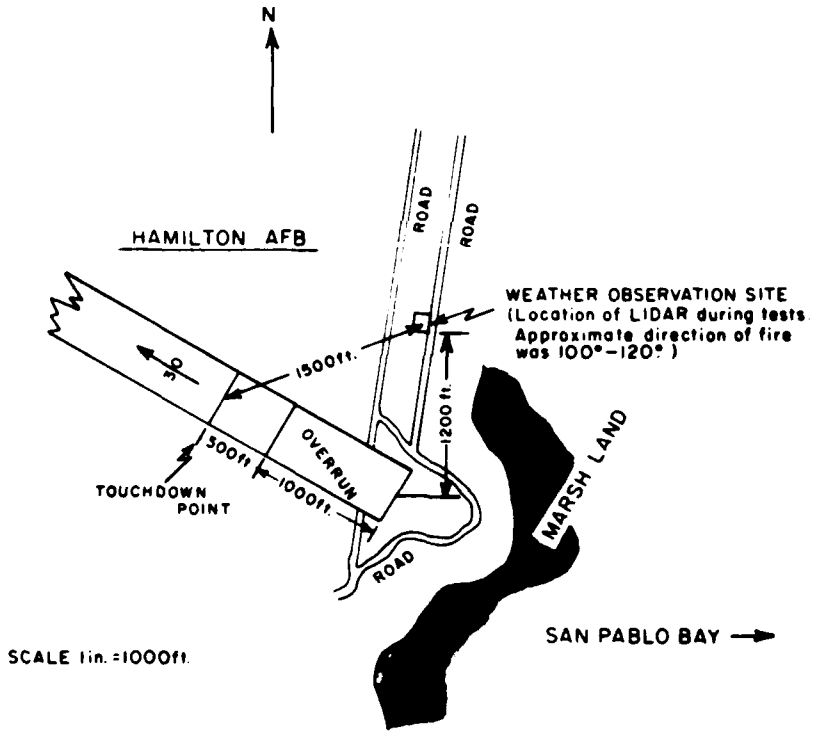

FIG. 1 LOCATION OF SRI LIDAR AT HAMILTON AFB RELATIVE TO TOUCHDOWN POINT AND TO SAN PABLO BAY

the Bay, an area characterized by low ceiling and visibility, and extends six miles, with a 2.5-degree slope, to the point of touchdown. The Air Weather Service observing station and a rotating-beam ceilometer are located near touchdown--i.e., as near as possible to the area of deteriorating ceiling and visibility conditions (see Fig. 1). However, even at this forward location, ceiling and visibility conditions are often quite different from those encountered by incoming aircraft over the marshes and open water.

At the request of the base commander and the weather squadron commander, SRI considered the application of lidar to their special problem of remotely measuring ceiling and visibility along the landing approach path. The field experiment could not involve a large-scale effort, and therefore the collected data are incomplete in many respects. Consequently, analyses and discussions of the data presented in this report must be considered exploratory.

The manner in which the lidar data were collected and analyzed is discussed in Sec. II. Results of the hand analyses are presented in Sec. III. Computer techniques to numerically process lidar data related to cloud ceiling and visibility are discussed in Sec. IV.

The potential application of lidar to remote measurements of ceiling conditions is considered promising, particularly in view of the future availability of higher-performance lidars.

II METHOD OF OBSERVATION AND DATA ANALYSIS

The SRI Mark V pulsed ruby lidar, details of which are given in Table I, was transported to Hamilton AFB and was placed next to the

Table I

CHARACTERISTICS OF SRI MARK V RUBY LIDAR

Transmitter	
Laser	6X 3/8-inch ruby crystal, Brewster-angle one end, planar one end, uncoated
Q-switch	Rotating prism and saturable dye
Wavelength	6943 Å
Pulse length	15 ns
Peak power output	18 MW
Pulse energy output	0.27 Joule
Optics	6-inch Newtonian reflector telescope
Beamwidth	Approximately 0.3 mrad
PRF	Two per minute
Receiver	
Detector photomultiplier	14-stage RCA type 7265
Optics	6-inch Newtonian reflector telescope with adjustable field stop
Field of view	0.2 to 0.9 mrad
Bandpass	Approximately 17 Å

weather observing station and the rotating-beam ceilometer. Data related to cloud ceiling and visibility were collected by firing at a pulse rate frequency of one or two pulses per minute out across the Bay, parallel to the aircraft glide path (see Fig. 1). The elevation angle of the direction of firing was varied from zero to 65 degrees without change of azimuth. All data were obtained under the actual weather conditions that create the operational problems. The weather conditions that prevailed during the period of lidar operation are given in Table II. Lidar observations were made during the afternoon and evening of 8 January and during the forenoon of 9 January.

Table II

WEATHER CONDITIONS DURING LIDAR OBSERVATIONS AT HAMILTON AFB, CALIFORNIA

Weather Conditions	8 January 1968	9 January 1968
Cloud ceiling	700-800 ft	400-500 ft
Prevailing visibility	1-1 2 to 2-1/2 mi	1 4 to 1/2 mi
Obstruction to visibility	Fog, occasional light rain	Fog, light drizzle
Temperature	37°-38°F	39°-40°F

Each lidar firing was separately recorded by photographing the trace of received signal power vs. slant range (often called the backscatter signature) as it appeared on the oscilloscope ("A scope"). Interpretation of the recorded data is best explained with the aid of the lidar equation which can be written in the form

$$P_r(R) = P_T \frac{c\tau}{2} \frac{A_r}{R^2} \beta_{180}(R) T_c(R) \exp\left[-2\int_o^R \sigma(R')dR'\right] \qquad (1)$$

where

P_r - Power collected (at a given instant) by the primary receiver optics from atmospheric backscatter of laser energy

R = Range

P_T = Power transmitted into the atmosphere

c = Velocity of light

τ = Pulse duration (seconds)

A_r = Effective receiver area

$\beta_{180}(R)$ = Volume backscatter coefficient

$T_c(R)$ = Beam convergence factor

$\sigma(R)$ = Volume extinction coefficient

The above formulation assumes a constant energy density across the beam, randomly distributed scatterers within the effective scattering volume, and Bouguer's law of attenuation. When the beam convergence factor, T_c, is excluded, Eq. (1) is valid only at ranges beyond the point where the diverging transmitted beam of the non-coaxial lidar system is fully encompassed by the diverging receiver field of view. By including T_c, Eq. (1) can describe the behavior of the lidar return signal at close-in range. T_c varies between 0 (before beam interception) and 1 (at full beam convergence) and is a function of the specific lidar system used.

Figure 2 shows examples of lidar data obtained at three elevation angles. The received signal power (related to P_r) on a logarithmic scale is recorded vs. slant range (R) on a linear scale. The use of a logarithmic video amplifier in the receiver is almost essential in order to compress the wide dynamic range of the detector (typically four or more orders of magnitude) and to enable the received signal to be displayed on a single oscilloscope trace without loss of detailed information. The sweep speed of the oscilloscope in Fig. 2(b) and 2(c) is twice as fast (1 microsecond per division with a maximum recorded range of 1.5 km) as that in Fig. 2(a) (2 microseconds per division with a maximum recorded range of 3.0 km) in order to show the significant lidar "echoes" detected at the higher elevation angles in more detail. At close-in ranges (up to about 100 m) where the beam convergence factor

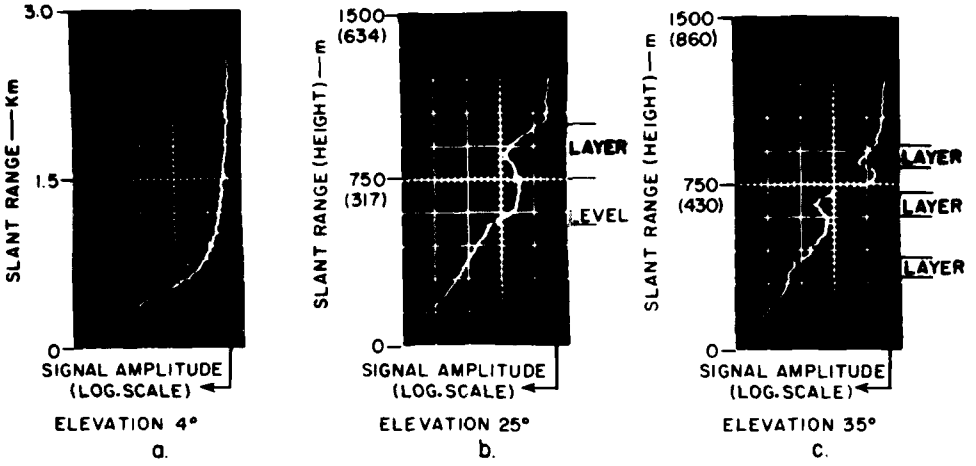

FIG. 2 SAMPLES OF LIDAR DATA OBTAINED AT HAMILTON AFB, CALIF., UNDER CONDITIONS OF LOW CEILING AND VISIBILITY

T_c dominates, the receiver output increases rapidly from zero as the diverging transmitted beam gradually merges with the diverging receiver field of view. The point of full beam convergence normally lies near the peak of the curve--i.e., near the point of maximum signal amplitude at the bottom of the photograph. In Fig. 2(a), the receiver output reaches a maximum near the point of full beam convergence at a range of 100 to 120 m, after which it falls as the distance to the fog particles producing the backscatter increases.

If large inhomogeneities such as cloud layers are present along the path, the strength of the return signal may suddenly increase and/or decrease as shown in Fig. 2(b) and 2(c). In the present experiment, a rapid increase in received power followed by a decrease is considered as an echo related to a cloud layer, while a single rapid decrease [Fig. 2(b)] is related to a level of large change in the transmitted signal attenuation. This large change in attenuation can arise from either a rapid increase or a rapid decrease in the optical density of the fog or clouds. Layers and levels observed by the lidar during one complete "scan" from the horizontal to the near vertical are analyzed

and related to the low cloud structure and the cloud ceiling as measured by the ceilometer.

Recorded data of received signal power vs. range obtained along the horizontal line of sight can be related to horizontal visibility while those obtained at low elevation angles [Fig. 2(a)] can be related to slant visibility. However, for correct application to visibility, the lidar data need to be processed numerically to extract the volume extinction coefficient, $\sigma(R)$, which is fundamental to the determination of visibility. Because of the limited scope of the Hamilton AFB experiment, the transfer characteristics of the receiver optics (including photomultiplier, logarithmic amplifier, and oscilloscope) could not be determined with the required accuracy. Therefore, values of received signal power could not be reliably transformed into absolute values of $P_r(R)$. Furthermore, examination of the lidar data after the experiment revealed that the very large backscatter signal from the fog at close-in range tended to saturate the receiver. This receiver saturation, in turn, caused a time-dependent discharge of photons ("after pulsing") which invalidates any computations based on the slope of the backscatter curves obtained at low elevation. In view of these difficulties no worthwhile analysis of lidar data in terms of horizontal and/or slant visibility is presented.

BLANK PAGE

III LIDAR OBSERVATIONS RELATED TO CLOUD CEILING

A. Hand Analysis of Available Data

Figures 3, 4, and 5 present the spatial distribution of the low-level cloud layers as observed with the lidar in the direction of San Pablo Bay during three separate time periods on 8 January 1968. The spatial distributions are obtained by firing the lidar at successive elevation angles from a maximum of 65 degrees down to the horizontal and analyzing along each direction of firing all echoes related to cloud layers and to levels of optical density change. Layers are indicated by solid bars and levels by solid triangles. Representative samples of individual lidar shots accompany each figure. Also indicated in each figure is the available surface-weather observation for the time closest to the period of the lidar data. Observed cloud-ceiling height (in hundreds of feet) is given by the ceilometer. Observed horizontal visibility is the so-called prevailing visibility defined as "the greatest visibility that is attained or surpassed throughout at least half of the horizon circle, not necessarily continuous."

Figures 3 through 5 show that under the prevailing weather conditions the lidar is capable of describing the low-cloud structure from the observation site out to a distance of 0.8 to 1.2 km (1/2 to 3/4 mi). This relatively limited range is due to the large attenuation of the lidar pulse energy along the slant paths through the fog at low elevation. During the evening, when the reported horizontal visibility increases from 1-1 2 to 2-1 2 miles, the range of lidar cloud-detection reaches the maximum of 3 4 mile. The cloud-ceiling height measured at the observation site by the rotating-beam ceilometer corresponds to the height of the lowest layer of lidar echoes obtained at high elevation angle.

Figure 3 shows a marked difference in the cloud structure between elevation angles larger and less than about 35 degrees. This difference probably arises from the fact that at high elevation angle the low-cloud

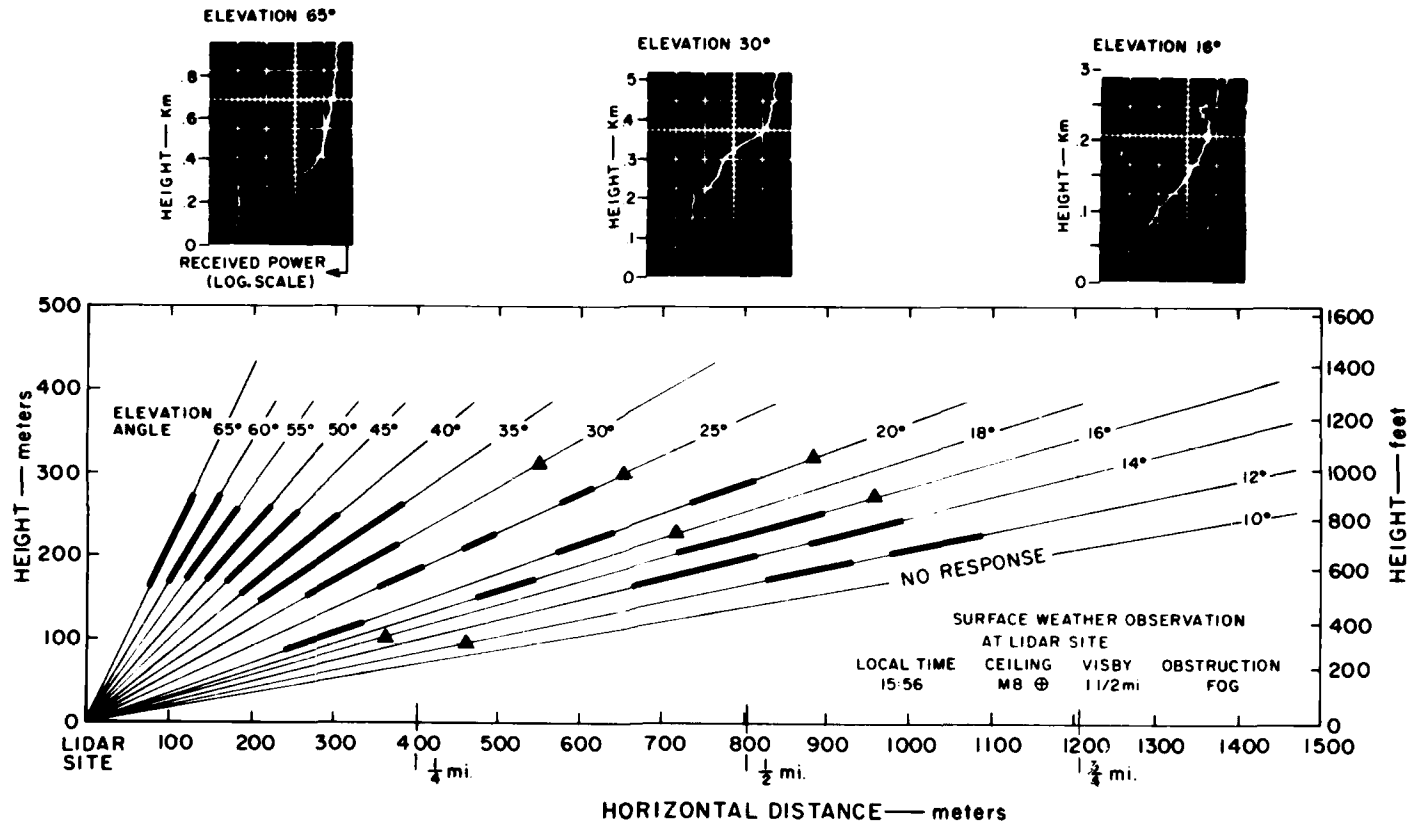

FIG. 3 SPATIAL DISTRIBUTION OF LOW CLOUDS DETECTED BY LIDAR AT HAMILTON AFB, CALIF., ON 8 JANUARY 1968, 15:26 - 15:54 LST. (Solid Bars: Cloud Layers; Solid Triangles: Levels of Optical Density Change)

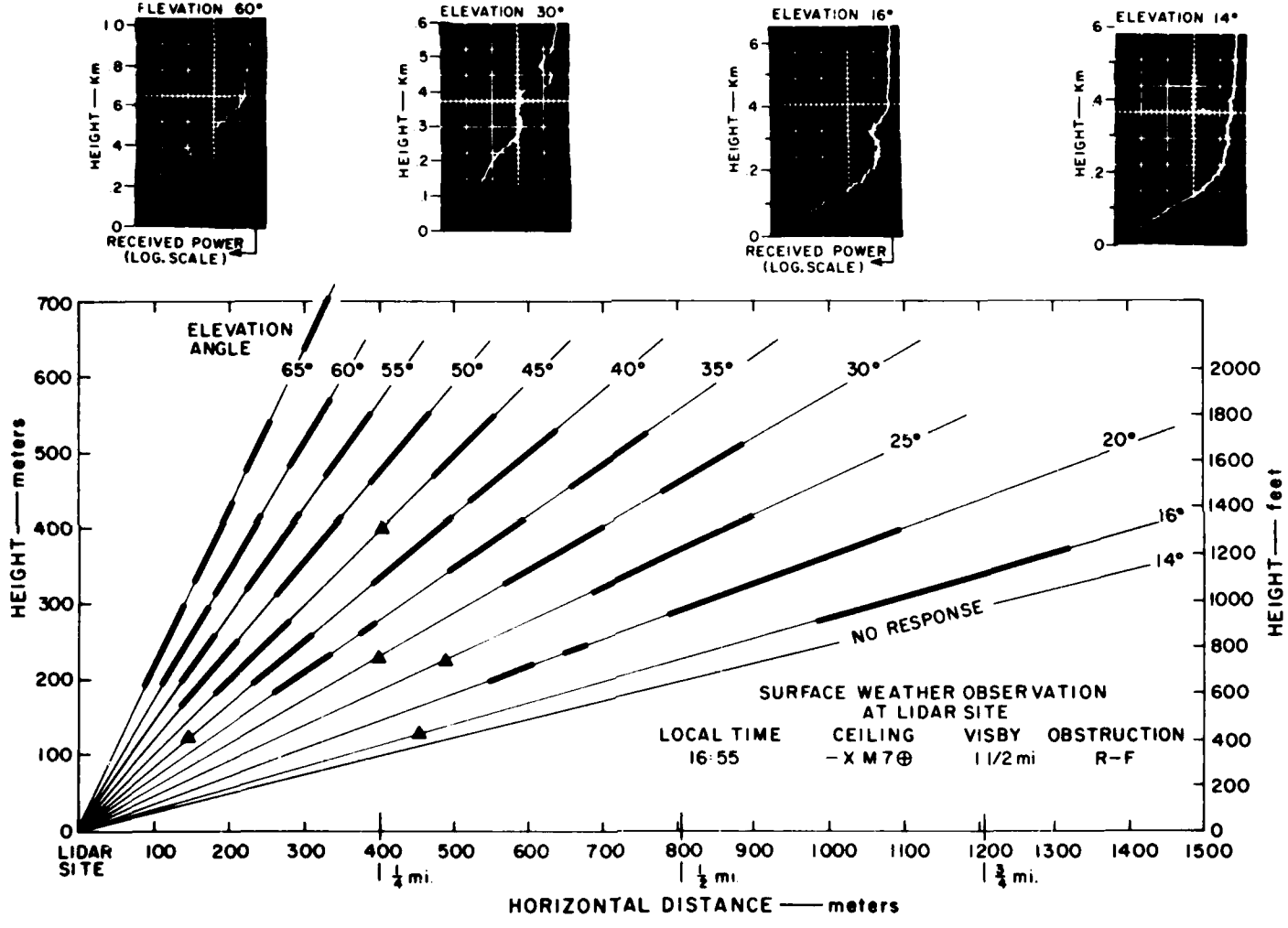

FIG. 4 SPATIAL DISTRIBUTION OF LOW CLOUDS DETECTED BY LIDAR AT HAMILTON AFB, CALIF., ON 8 JANUARY 1968, 16:41 - 16:51 LST. (Solid Bars: Cloud Layers; Solid Triangles: Levels of Optical Density Change)

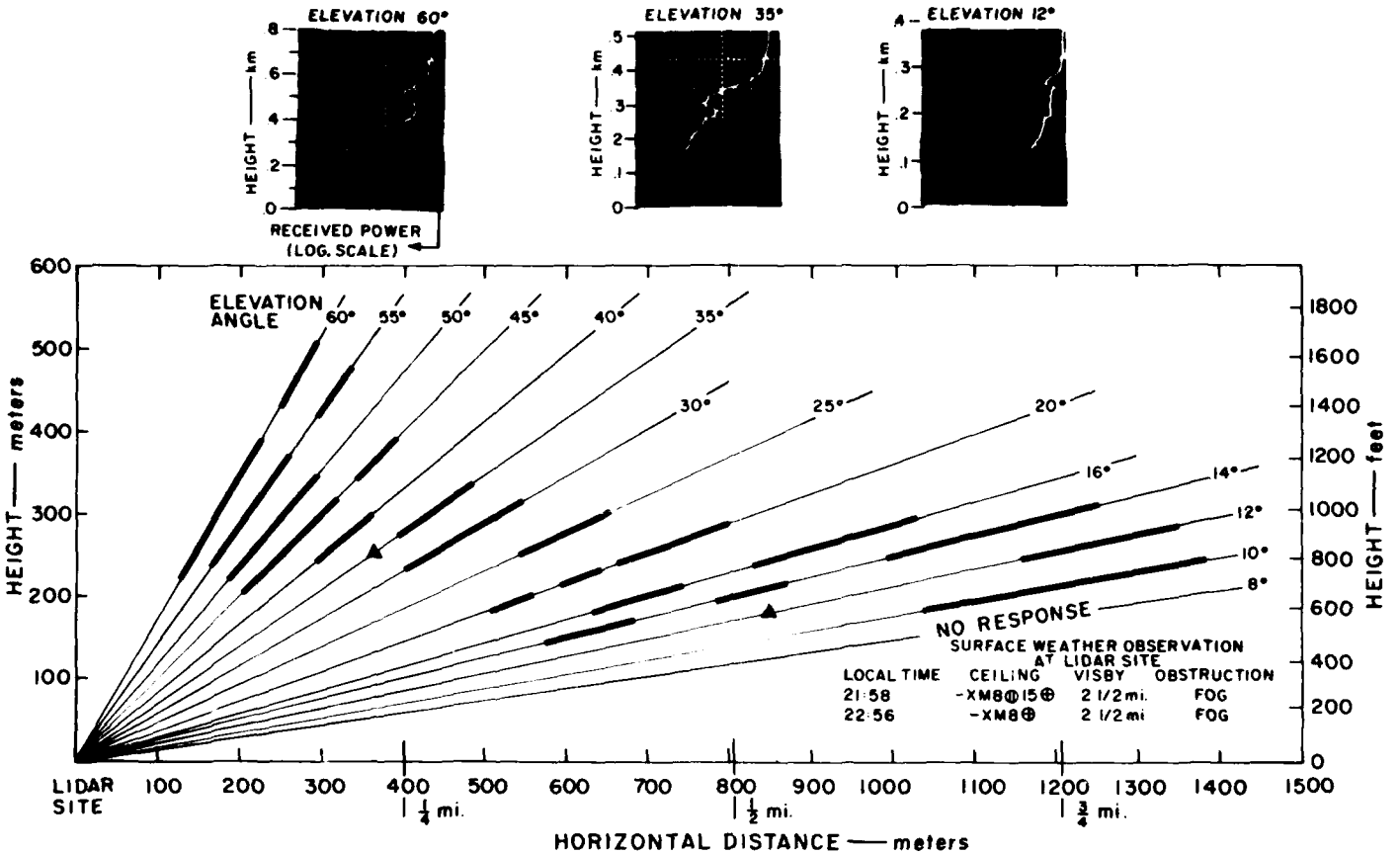

FIG. 5 SPATIAL DISTRIBUTION OF LOW CLOUDS DETECTED BY LIDAR AT HAMILTON AFB, CALIF., ON 8 JANUARY 1968, 22:22 - 22:31 LST (Solid Bars: Cloud Layers; Solid Triangles: Levels of Optical Density Change)

echoes are detected at close range, with a subsequent loss of resolution in the recorded lidar trace (see sample of individual lidar shot at 65 degrees elevation). Under such conditions a change in the sweep speed of the "A scope" must be used to "magnify" the lidar trace.

Figures 4 and 5 show that higher-level cloud layers are detected only at the high elevation angles, where the path length through the lower clouds and the fog is minimum. The ceilometer detected higher cloud layers only during the time period of Fig. 5 when the ceiling was broken.

Figures 6 and 7 illustrate the capability of the SRI ruby lidar to remotely monitor cloud-ceiling variations at a point distant from

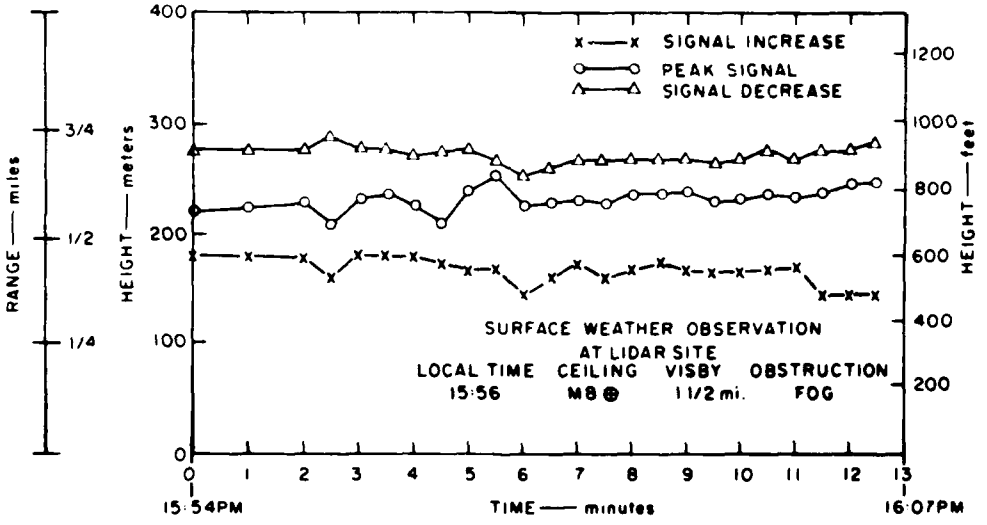

FIG. 6 TIME VARIATION OF LOW-CLOUD STRUCTURE MONITORED BY LIDAR AT 1 2 TO 3 4 MILE FROM THE LIDAR SITE AT HAMILTON AFB DURING AFTERNOON OF 8 JANUARY 1968

the observation site. Figure 6 shows a 12-minute time section of the low-level cloud structure over the Bay at points approximately 1/2 to 3/4 mile from the lidar site (14 degrees elevation angle) during the

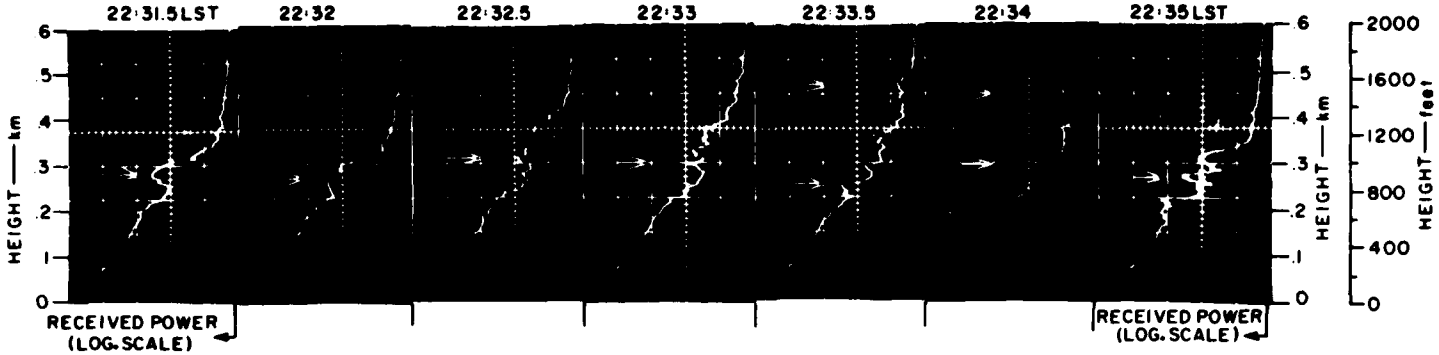

AVAILABLE SURFACE WEATHER OBSERVATIONS AT LIDAR SITE	LOCAL TIME	CEILING	VISBY	OBSTRUCTION
	21:58	-XM8⊕15⊕	2 1/2mi.	FOG
	22:56	-XM8⊕	2 1/2mi.	FOG

FIG. 7 TIME VARIATION OF OBSERVED LIDAR PROFILES RELATED TO THE LOW-CLOUD STRUCTURE AT 1/4 MILE FROM THE LIDAR SITE AT HAMILTON AFB DURING EVENING OF 8 JANUARY 1968

afternoon of 8 January. The time period corresponds to that of Fig. 3. The levels of signal increase, peak signal return, and signal decrease monitored at time intervals of about 30 seconds are indicated and joined by straight-line segments to portray the time variation of a 100-meter-thick low-cloud layer. Practically no change with time is evident. Conditions at the remote locations are nearly identical to those "overhead" at the observation site, the height of the peak signal return being nearly identical to the ceiling height given by the ceilometer. Figure 7 shows the low-cloud configuration as recorded with the lidar at a point about 1 4 mile from the observation site (30 degrees elevation angle) during a time period of 3 to 4 minutes. The data are part of the series analyzed in Fig. 5 and were obtained on the evening of 8 January. The surface weather observation before and after the period of lidar observations is indicated. The lowest cloud layer detected by the lidar (indicated in Fig. 7 by arrows) closely corresponds to the 800-ft (244 m) ceiling measured by the ceilometer. On two occasions (22:33.5 LST and 22:34 LST) the lidar data show the upper (1500 ft) cloud layer detected by the ceilometer at 21:58 LST. Thus, the density variations in the lower clouds apparent from the lidar data are recorded by the ceilometer also.

During the morning of 9 January, very low ceiling and visibility prevailed. Up to 11:57 LST the sky cover remained overcast, with the cloud base varying between 400 ft (122 m) and 500 ft (152 m). The prevailing horizontal visibility remained around 1 2 mile (0.8 km) in light drizzle and fog (see Table II). At 11:57 LST, clouds became broken. Figure 8 illustrates some typical lidar backscatter profiles obtained throughout the morning at 30 degrees elevation. The rapid decrease in return signal amplitude observed at a height near 150 m (492 ft) at 11:53 LST must be interpreted as due to a rapid increase in optical density, since this height corresponds to that of the cloud ceiling measured by the ceilometer at the lidar site. Furthermore, at 11:50 LST an airborne weather observer* reported a 400-ft (140-m)

*Capt. R. H. Hedenberg, Commander, Det. 9, 35th Weather SQ., Hamilton AFB.

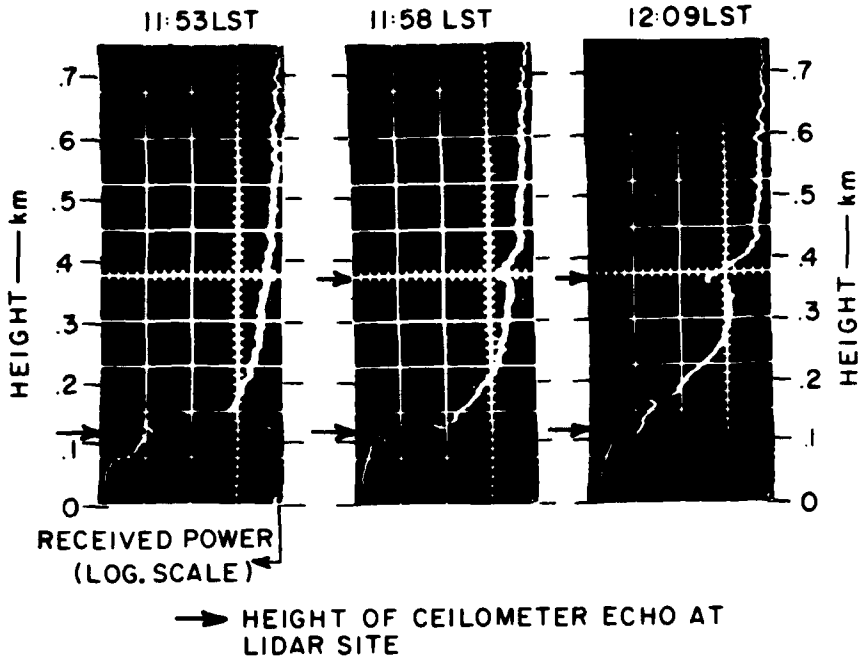

FIG. 8 SAMPLES OF LIDAR DATA OBTAINED AT 30 DEGREES ELEVATION AT HAMILTON AFB ON 9 JANUARY 1968

cloud ceiling at 1 mile from touchdown and indicated that clouds extended vertically to at least 2000 ft (610 m). Near 12 o'clock noon, however, this dense lower layer became transparent, as evident by the appearance of a cloud echo near 360 m in the lidar profile of 11:58 LST. The higher-level cloud layer was also detected by the ceilometer at the lidar site and was first reported in the surface weather observation at 11:57 LST.

Figure 9 shows the spatial extent of the significant layers and levels detected by the lidar shortly after noon. The lowest-altitude signals correspond to the 400-ft broken-cloud layer indicated by the ceilometer. Agreement between ceilometer and lidar data extends to 1200 ft.

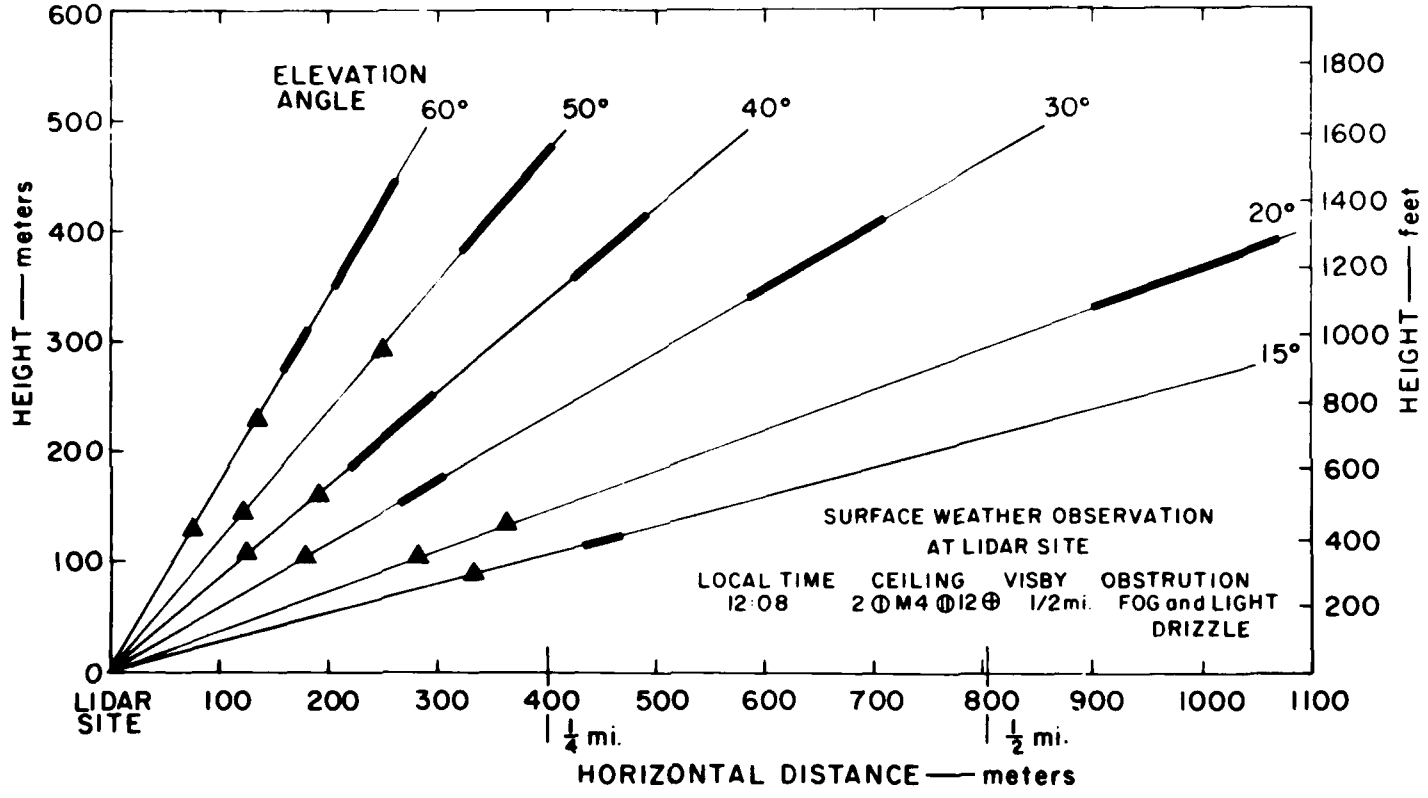

FIG. 9 SPATIAL DISTRIBUTION OF LOW CLOUDS OBSERVED BY LIDAR AT HAMILTON AFB, CALIF., ON 9 JANUARY 1968, 12:07 - 12:11 LST (Solid Bars: Cloud Layers; Solid Triangles: Levels of Optical Density Change)

B. Discussion

The data samples analyzed in Figs. 3 through 9 demonstrate the advantages and limitations of the lidar in the description of the low-level cloud structure under adverse weather conditions. Because of its pulsed nature, the lidar can provide a vertical density profile through the low-level clouds and, furthermore, because of its ability to operate under variable elevation and azimuth, can accurately describe the spatial distribution of the cloud ceiling. A most useful feature of the lidar is its ability to monitor the cloud-ceiling conditions at a location that is remotely situated with respect to the lidar site. Under the weather conditions that prevailed during the Hamilton AFB experiment, the lidar could accurately monitor the cloud ceiling at a point 1/2 to 3/4 mile from touchdown point.

A replacement of the ceilometer by a lidar would greatly expand the range of information on cloud-ceiling height and low-cloud structure that could be obtained. On the other hand, the lidar data show a high spatial correlation with the spot information provided by the ceilometer. Under the conditions of fog and drizzle that prevailed during the experiment, the ceilometer reading appeared equally valid for locations up to 1/2 to 3/4 mile away. With the experimental lidar used, it was disappointing that the maximum range at which the low clouds could be accurately described remained well below the 1-mile mark. During the conditions of fog and light rain or light drizzle that prevailed during the experiment, the long slant paths at elevation angles below 10 to 15 degrees rapidly attenuated the ruby lidar pulse energy down to the noise level. Improvement in the range of cloud-mapping capability can be expected in the future by further narrowing the transmitted lidar beam and by introducing higher-power output.

IV COMPUTER TECHNIQUES FOR ANALYZING LIDAR DATA RELATED TO CLOUD CEILING AND VISIBILITY*

This section describes methods of producing computer-analyzed cross sections of atmospheric optical parameters from an input of digitized lidar data. Because of the above-mentioned instrumental uncertainties with respect to receiver transfer characteristics and overloading, results of the numerical analyses must be evaluated in terms of relative variations rather than absolute values--i.e., application is to cloud ceiling rather than to visibility.

A. Computer Analysis of Data Sample

In order to digitize the recorded lidar data, Polaroid prints of the oscilloscope-displayed lidar signatures, such as shown in Fig. 2, are projected with a magnification of 5 power onto a screen of a scaling machine (digitizer) that records on IBM cards the (X, Y) coordinates of a movable crosshair. The operator records (X, Y) values of all inflection points on a lidar recorded signature that, when joined by straight lines, provide a digitized representation of the signature. The (X, Y) representation of each lidar signature thus obtained constitutes the input for a computer program, which, by use of the digitizer calibration and the beam elevation angle, converts the (X, Y) values into a matrix of oscilloscope deflection (output voltage) of the data points and a matrix of position of the data points. Such output data from multiple laser firings obtained as the lidar scans from the horizontal to the near vertical are then fed into a grid-point-analysis program.† This program assigns a value of the dependent variable (in this

---

*Part of the work reported on in this section was supported by Stanford Research Institute (see Acknowledgments) and SRI Project 7165. (See Ref. 1. References are listed at the end of the report).

†Developed by Mr. R. L. Mancuso of the Aerophysics Laboratory.

case, oscilloscope deflection in volts) to each grid point of a predetermined grid in the vertical plane of observation. Values to individual grid points are assigned on the basis of the five data points nearest to the grid point with the aid of a distance-weighting factor as well as a vector weight defined in the radial direction (which gives more weight to data from a single lidar profile) or in the horizontal direction (which gives weight to existing conditions of horizontal stratification).

Figure 10(a) shows the results of this type of computer analysis using the lidar data observed during the evening of 8 January 1968 (22:22-22:31 LST). The analysis is prepared from the data of 18 individual lidar profiles obtained at elevation angles ranging from zero to 60 degrees. In Fig. 10 and in all subsequent figures, coordinate axes and isopleths are drawn by hand. In order to supply as much input data as possible to the grid-point-analysis program, data points intermediate to the inflections were obtained by linear interpolation within the computer program. Minimum distance between signature data points was 25 m. The oscilloscope-deflection analysis of Fig. 10(a) provides a field that is representative of atmospheric scattering activity. The layer of maximum scattering activity at a height of 250 to 275 m is related to the level of low clouds shown in the hand analysis of the same date in Fig. 5.

It is possible to transform the voltage field of Fig. 10(a) into a parameter field more representative of atmospheric conditions and perhaps, in the case of ideal data, into a field of extinction coefficients from which the meteorological range or the "visibility" along any given path (such as along an aircraft landing approach path) may be inferred. Referring to Eq. (1), the lidar equation, a convenient range-corrected quantity, in dB notation, can be defined as:

$$S(R) = 10 \log \frac{P(R)R^2}{P(R_o)R_o^2} = 10 \log \frac{\beta_{180}(R)T_a^2(R)T_c(R)}{\beta_{180}(R_o)T_a^2(R_o)T_c(R_o)} \qquad (2)$$

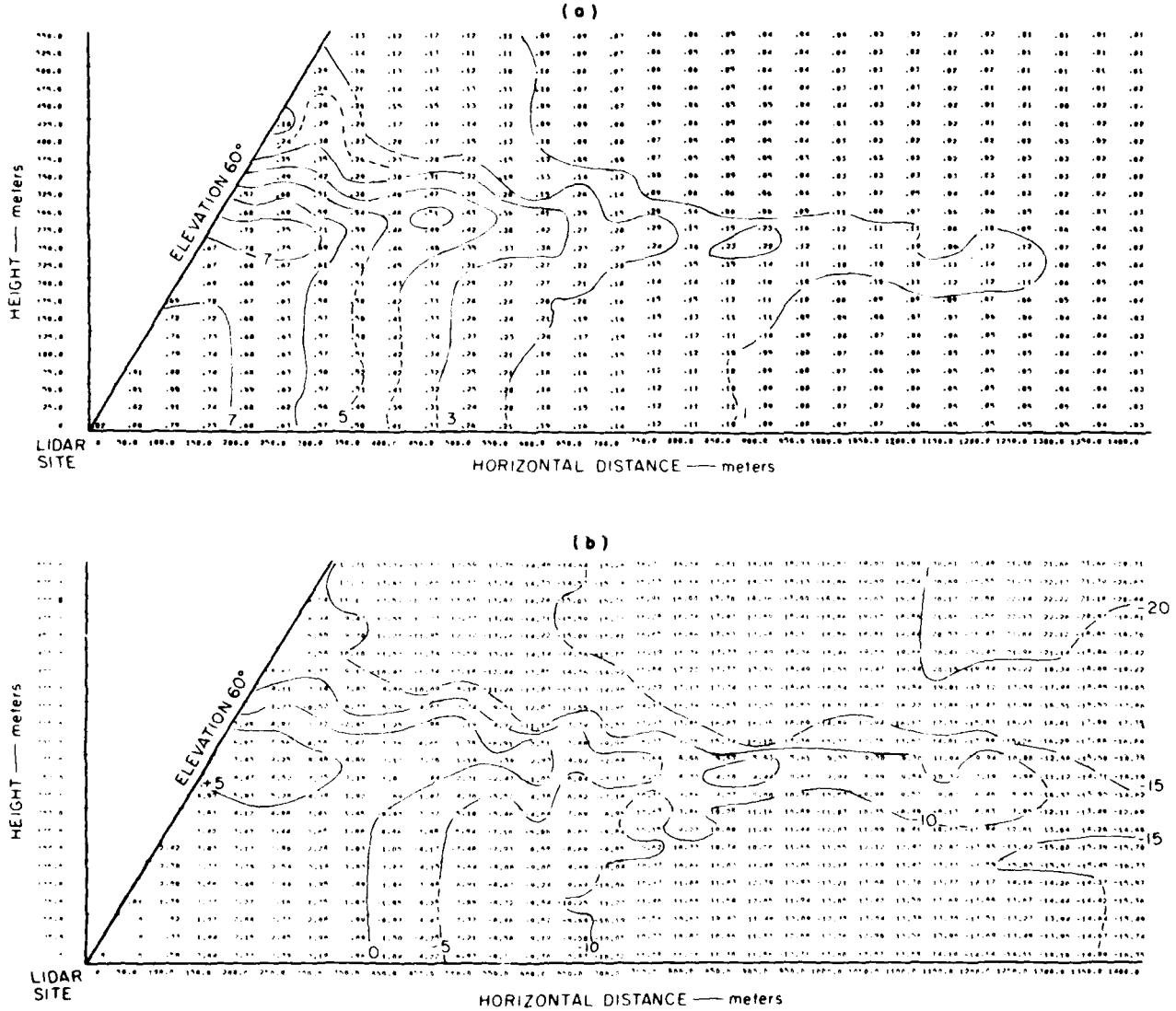

FIG. 10 COMPUTER PRINTOUT FOR GRID-POINT ANALYSIS OF (a) OSCILLOSCOPE-DEFLECTION IN RELATIVE VOLTAGE AND (b) S-FUNCTION IN RELATIVE dB, IN THE VERTICAL PLANE OF LIDAR OBSERVATION. (HAMILTON AFB, 8 JANUARY, 1968, 22:22 - 22:31 LST)

where R_o is a reference range on each lidar trace and

$$T_a(R) = \exp - \int_o^R \sigma(R')\, dR'$$

is the one-way atmospheric transmission over the range R. All other terms are as defined previously. Again using the lidar data observed during the evening of 8 January, a grid-point analysis of S(R) was obtained in the following manner. From a relative calibration of the nonlinear response of the Mark V ruby lidar receiver (including photomultiplier, logarithmic amplifier and oscilloscope) estimated to be valid for the conditions of the Hamilton AFB experiment, a polynomial operator was defined by means of which the computer transforms the output-voltage field of Fig. 10(a) into a field of relative light $[P_r(R)]$ incident on the primary receiver optics. Using the first data point on each of the 18 lidar observations as the reference range R_o, Fig. 10(b) shows the computer output of the S-function field thus obtained. Large increases and decreases with height correspond to cloud layers. A comparison with the qualitative analysis of the same data shown in Fig. 5 clearly indicates the practicability of this computer-produced parameter field for cloud-ceiling determination.

The derivative of S(R) over the region of full beam convergence ($T_c = 1$) may be expressed as:

$$\frac{dS}{dR} = 4.34 \frac{1}{\beta} \frac{d\beta}{dR} - 8.7\sigma \qquad (3)$$

where the subscript 180 and the range-dependence notation (R) have been omitted. A closed-form solution for the optical parameters β and σ requires additional information on the scattering properties of the atmosphere or on a backscatter-extinction relation. When the backscatter coefficient, $\bar{\beta}$, is independent of range, as is the case in a homogeneous scattering medium, the extinction coefficient between deflection points of S(R) is given by:

$$\bar{\sigma} = - \frac{1}{8.7} \frac{\Delta S}{\Delta R} \qquad (4)$$

Figure 11(a) presents a computer output of the grid-point analysis of $\bar{\sigma}$ over the complete field of Fig. 10. Negative values (shaded) and large positive values (unshaded) represent areas where the received lidar signal sharply increases and decreases, respectively. Beyond the range of full beam convergence, these areas correspond to areas of non-constant backscatter and allow inferences as to the levels of low-cloud layers analyzed in Fig. 5. Thus, the stratus clouds are clearly indicated in this computer analysis of the signature slope, even though the initial assumption of a constant β is obviously unreal. The presence of horizontally-extensive higher clouds is suggested by the areas of negative values (signal increase) at 500 m. The hand analysis of Fig. 5 shows these clouds only in the high-elevation lidar data. Thus, the computer is capable of analyzing small changes in signature slope that escape the eye.

A solution to Eq. (3) for the optical parameters β and σ is possible when the existing relation between these quantities is known. Fenn,[3] using the data of Barteneva,[2] and Curcio and Knestrick[4] have shown that a relation such as

$$\frac{d \ln \beta}{d \ln \sigma} = \text{constant} = k_2 \qquad (5)$$

is valid within 20 to 30 percent for extinction coefficients between 0.01 km^{-1} and 1.0 km^{-1} when employing a broad spectral source. Assuming such a relation to be valid for the conditions of this experiment, substitution of Eq. (5) into Eq. (3) yields a first-order nonlinear differential equation:

$$\frac{d\sigma}{dR} - C_1 \frac{dS}{dR} \sigma - C_2 \sigma^2 = 0$$

where $C_1 = 1 - 4.34\ k_2$ and $C_2 = 2\ k_2$. The transform $\tau = 1/\sigma$ reduces this differential equation to the linear form:

$$\frac{d\tau}{dR} + C_1 \frac{dS}{dR} \tau + C_2 = 0 \qquad (6)$$

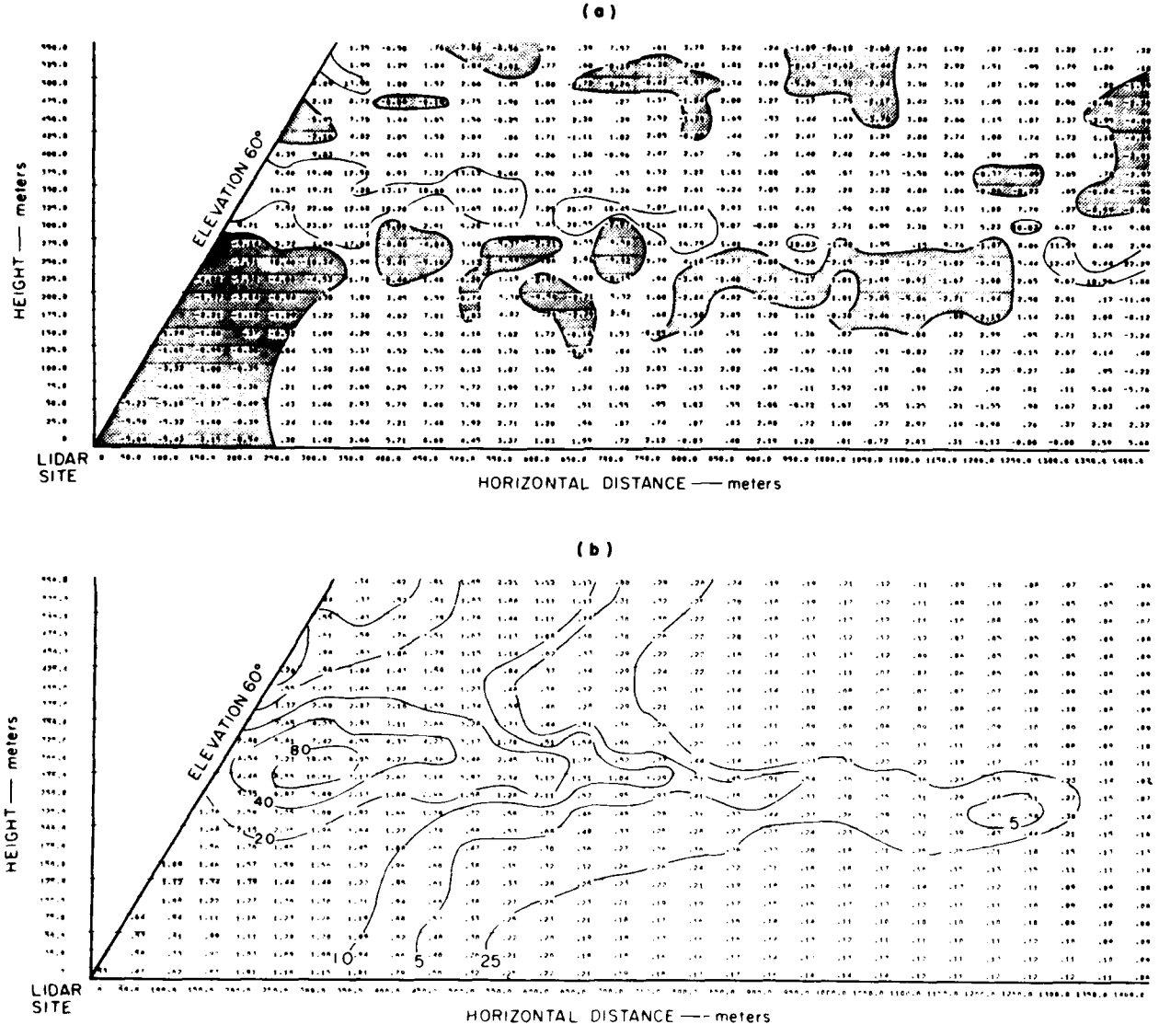

FIG. 11 COMPUTER PRINTOUT FOR GRID-POINT ANALYSIS OF (a) $\bar{\sigma}$ IN UNITS OF km^{-1} ASSUMING CONSTANT β, AND (b) $\bar{\sigma}$ IN UNITS OF km^{-1} ASSUMING $\beta \quad k_1 \sigma^{1.4}$ IN THE VERTICAL PLANE OF LIDAR OBSERVATION. (HAMILTON AFB, 8 JANUARY 1968, 22:22 - 22:31 LST)

for which the solution may be written as:

$$\sigma(R) = e^{C_1 S(R)}\left[C_I - C_2 \int_R e^{C_1 S(R')}\, dR'\right]^{-1} \qquad (7)$$

where C_I is the constant of integration. The derivative of S(R), which is formed by straight line segments between digitized lidar-signature inflection points, is not unique at these points--i.e., S(R) is a piecewise differentiable function. Thus, in addition to the requirement of a boundary value, the integration constant C_I must be re-evaluated for each S(R) line segment. Solution for multiple traces requires a boundary value for each trace or correction and or assumptions on lidar variable parameters between traces. The method used in the analysis of the present lidar data was to obtain a boundary value of extinction coefficient from the slope technique for part of a signature for which the backscatter was thought to be constant with range. Solution was then taken along this trace in the direction of the lidar. Boundary values of σ at the initial data point (range R_o) for each additional trace were derived assuming unity transmission of the lidar energy to these data points and the initial value of σ from the trace containing the boundary point. Extinction coefficients were then evaluated for each data point in the field. A value of 1.4 was assigned to the constant k_2. Such a value probably underestimates the attenuation of the lidar energy and thus increases the probability of a valid solution at regions of large signal variations along the lidar signature. The validity of the solution field is determined by re-deriving the S functions from the right-hand term of Eq. (2) from evaluated quantities.

Figure 11(b) presents the grid-point analyses of the $\bar{\sigma}$ field obtained. As in the previous computer analyses, the level of the low clouds is clearly shown by large values and large vertical gradients of $\bar{\sigma}$. By comparison with Fig. 10(b), it is clear that some of the attenuation effect has been removed from the data field. However, the non-horizontal isopleths indicate that additional attenuation should be accounted for by employing a smaller value of k_2 or a larger value of the boundary extinction coefficient. Further experimentation along

these lines was not considered justified because of the limited quantity and quality of the data. The real merit of a derived σ-field is that transmission along any line segment defined by two points in the field may be evaluated and thus slant-range visibilities inferred.

B. Discussion

Figures 10 and 11 show the operational feasibility of describing the spatial distribution of cloud ceiling and low-cloud structure with a lidar-electronic computer combination. The results shown are not considered optimum since they depend on several assumptions that may be relaxed or altered through further investigations. The primary uncertainty is the validity of the assumed β-σ relation, which enables the solution of Eq. (3). It is suggested that in future experiments of the type described in this report, the neodymium laser be used because of its broader spectral energy (200 Å) in comparison to that of the ruby laser. The broad spectral characteristic gives more validity to assuming a β-σ relation (Twomey and Howell, Ref. 5). Also necessary is some further research in the numerical application of Eq. (7). For example, various boundary values can be evaluated by using a completely calibrated lidar or by using an extinction coefficient derived from the return of the lidar energy from a ground-based target of known reflectivity (Allen et al., Ref. 6)

V CONCLUSIONS AND RECOMMENDATIONS

This study covers a limited experiment in the use of lidar for the determination of ceiling and visibility. The conditions during the experiment, although ideal from a meteorological point of view, were by no means optimum in terms of equipment or experimental procedures. For example, the use of the neodymium version of the Mark V lidar, capable of firing every 4 to 5 seconds would have been preferable; also more complete calibration and reference-measurement procedures are desirable. However, the results demonstrate a real potential of lidar for use in operational determinations of aircraft landing visibility conditions.

It is evident that the lidar can obtain cloud ceiling, even when the cloud base is diffuse, at locations distant from the point of observation. At Hamilton AFB it was possible to obtain detailed information on the cloud conditions at locations along the approach path, where, because of the marshes and open water, conventional ceilometers could not be operated.

The possibility of processing lidar observations to obtain quantitative data on the extinction coefficient--i.e., the optical parameter significant to "visibility" determinations--has been explored with indications that operationally useful computer-produced analyses are feasible. The objective determination of a cross section showing a field of values that are related to atmospheric scattering activity and that portray conditions of low-cloud ceiling and reduced horizontal visibility is considered to be a major advance in this problem area, and one that offers hope of eventually being able to infer "slant visibility" for aircraft landing operations.

It is obvious, however, that much remains to be done. For simple graphical description of the cloud base, further work is necessary on the physical interpretation of inflections on the lidar signature, and also on the technique of processing and displaying data. The conversion of lidar observations to digital form for computer processing, and the computational solutions themselves also need further development.

Progress in both these areas would involve additional experimental and development programs. The programs should be geared toward obtaining optimum techniques of data processing and display that can lead to the design of practical instrumentation for routine operational use.

ACKNOWLEDGMENTS

Part of the costs of carrying out the observational program at Hamilton AFB were met by Stanford Research Institute. The Institute also supported research into the computer processing of lidar data, results of which are used in this study.

The cooperation and hospitality received from Col. Harry W. Shoup, USAF, Commander 78th Fighter Wing, Hamilton AFB and from Col. Leroy C. Iverson, USAF, Commander 35th Weather Squadron and Lt. Col. Milton Plattner are gratefully acknowledged. Special credit is due to Capt. R. H. Hedenberg, USAF, Commander, Det. 9, 35th Weather Squadron, for his assistance throughout the project.

REFERENCES

1. R. J. Allen, E. E. Uthe, and W. E. Evans, "Tactical Considerations of Atmospheric Effects on Laser Propagation," Quarterly Status Report 1, Contract N00019-68-C-0201, SRI Project 7165, Stanford Research Institute, Menlo Park, California (May 1968).

2. R. W. Fenn, "Correlation Between Atmospheric Backscattering and Meteorological Visual Range," Appl. Opt., Vol. 5, No. 2, pp. 293-295 (February 1966).

3. O. D. Barteneva, "Scattering Functions of Light in Atmospheric Boundary Layer," Bull. (Izvestia) Aca. Sc. USSR, No. 12 (1960).

4. J. A. Curcio and G. L. Knestrick, "Correlation of Atmospheric Transmission with Backscattering," J. Opt. Soc. Am., Vol. 48, No. 10, pp. 686-689 (1958).

5. S. Twomey and H. B. Howell, "The Relative Merit of White and Monochromatic Light for the Determination of Visibility by Backscattering Measurements," Appl. Opt., Vol. 4, No. 4, pp. 501-506 (April 1965).

6. R. J. Allen, E. E. Uthe, and J. W. Oblanas, "Tactical Considerations of Atmoshperic Effects on Laser Propagation," Quarterly Status Report 3, Contract N00019-67-C-0270, SRI Project 6540, Stanford Research Institute, Menlo Park, California (November 1967).

UNCLASSIFIED
Security Classification

DOCUMENT CONTROL DATA - R&D

(Security classification of title, body of abstract and indexing annotation must be entered when the overall report is classified)

1. ORIGINATING ACTIVITY *(Corporate author)*
Stanford Research Institute
Menlo Park, California 94025

2a. REPORT SECURITY CLASSIFICATION
UNCLASSIFIED

2b. GROUP
N/A

3. REPORT TITLE
ANALYSIS OF LIDAR DATA OBTAINED UNDER CONDITIONS OF LOW CEILING AND VISIBILITY

4. DESCRIPTIVE NOTES *(Type of report and inclusive dates)*
Scientific Interim

5. AUTHOR(S) *(Last name, first name, initial)*
William Viezee
Edward E. Uthe

6. REPORT DATE	7a. TOTAL NO. OF PAGES	7b. NO. OF REFS
August 1968	44	6

8a. CONTRACT OR GRANT NO.
Contract No. F 19628-68-C-0021

b. PROJECT, TASK, WORK UNIT NOS.
6670-02-01

c. DOD ELEMENT
62405394

d. DOD SUBELEMENT
681000

9a. ORIGINATOR'S REPORT NUMBER(S)
Scientific Report No. 1
SRI Project 6963

9b. OTHER REPORT NO(S) *(Any other numbers that may be assigned this report)*
AFCRL-68-0522

10. AVAILABILITY/LIMITATION NOTICES
(1) Distribution of this document is unlimited. It may be released to the Clearinghouse, Department of Commerce, for sale to the general public.

11. SUPPLEMENTARY NOTES
TECH, OTHER

12. SPONSORING MILITARY ACTIVITY
Air Force Cambridge Research Laboratories (CRE)
L. G. Hanscom Field
Bedford, Massachusetts 01730

13. ABSTRACT

Lidar (laser radar) data obtained at Hamilton AFB, California, under conditions of low ceiling and visibility are analyzed by hand and by electronic computer to explore the operational utility of lidar in cloud ceiling and visibility determination for aircraft landing operations. Hand analyses of the data show the ability of the lidar to describe the spatial configuration of the low-cloud structure with respect to touch-down point. The problems inherent in evaluation of lidar observations are discussed, and initial approaches to quantitative solutions by computer are presented. It is demonstrated that operationally useful information on the ceiling and visibility conditions contained in the hand analyses can be presented by digitizing the lidar data and subjecting these data to computer analysis.

DD FORM 1 JAN 64 1473

UNCLASSIFIED
Security Classification

UNCLASSIFIED

Security Classification

14. KEY WORDS	LINK A		LINK B		LINK C	
	ROLE	WT	ROLE	WT	ROLE	WT
Laser Radar Lidar Cloud ceiling measurements Visibility determination Ceilometer						

INSTRUCTIONS

1. **ORIGINATING ACTIVITY**: Enter the name and address of the contractor, subcontractor, grantee, Department of Defense activity or other organization *(corporate author)* issuing the report.

2a. **REPORT SECURITY CLASSIFICATION**: Enter the overall security classification of the report. Indicate whether "Restricted Data" is included. Marking is to be in accordance with appropriate security regulations.

2b. **GROUP**: Automatic downgrading is specified in DoD Directive 5200.10 and Armed Forces Industrial Manual. Enter the group number. Also, when applicable, show that optional markings have been used for Group 3 and Group 4 as authorized.

3. **REPORT TITLE**: Enter the complete report title in all capital letters. Titles in all cases should be unclassified. If a meaningful title cannot be selected without classification, show title classification in all capitals in parenthesis immediately following the title.

4. **DESCRIPTIVE NOTES**: If appropriate, enter the type of report, e.g., interim, progress, summary, annual, or final. Give the inclusive dates when a specific reporting period is covered.

5. **AUTHOR(S)**: Enter the name(s) of author(s) as shown on or in the report. Enter last name, first name, middle initial. If military, show rank and branch of service. The name of the principal author is an absolute minimum requirement.

6. **REPORT DATE**: Enter the date of the report as day, month, year, or month, year. If more than one date appears on the report, use date of publication.

7a. **TOTAL NUMBER OF PAGES**: The total page count should follow normal pagination procedures, i.e., enter the number of pages containing information.

7b. **NUMBER OF REFERENCES**: Enter the total number of references cited in the report.

8a. **CONTRACT OR GRANT NUMBER**: If appropriate, enter the applicable number of the contract or grant under which the report was written.

8b, 8c, & 8d. **PROJECT NUMBER**: Enter the appropriate military department identification, such as project number, subproject number, system numbers, task number, etc.

9a. **ORIGINATOR'S REPORT NUMBER(S)**: Enter the official report number by which the document will be identified and controlled by the originating activity. This number must be unique to this report.

9b. **OTHER REPORT NUMBER(S)**: If the report has been assigned any other report numbers *(either by the originator or by the sponsor)*, also enter this number(s).

10. **AVAILABILITY/LIMITATION NOTICES**: Enter any limitations on further dissemination of the report, other than those imposed by security classification, using standard statements such as:

(1) "Qualified requesters may obtain copies of this report from DDC."

(2) "Foreign announcement and dissemination of this report by DDC is not authorized."

(3) "U. S. Government agencies may obtain copies of this report directly from DDC. Other qualified DDC users shall request through

_____."

(4) "U. S. military agencies may obtain copies of this report directly from DDC. Other qualified users shall request through

_____."

(5) "All distribution of this report is controlled. Qualified DDC users shall request through

_____."

If the report has been furnished to the Office of Technical Services, Department of Commerce, for sale to the public, indicate this fact and enter the price, if known.

11. **SUPPLEMENTARY NOTES**: Use for additional explanatory notes.

12. **SPONSORING MILITARY ACTIVITY**: Enter the name of the departmental project office or laboratory sponsoring *(paying for)* the research and development. Include address.

13. **ABSTRACT**: Enter an abstract giving a brief and factual summary of the document indicative of the report, even though it may also appear elsewhere in the body of the technical report. If additional space is required, a continuation sheet shall be attached.

It is highly desirable that the abstract of classified reports be unclassified. Each paragraph of the abstract shall end with an indication of the military security classification of the information in the paragraph, represented as *(TS), (S), (C), or (U)*.

There is no limitation on the length of the abstract. However, the suggested length is from 150 to 225 words.

14. **KEY WORDS**: Key words are technically meaningful terms or short phrases that characterize a report and may be used as index entries for cataloging the report. Key words must be selected so that no security classification is required. Identifiers, such as equipment model designation, trade name, military project code name, geographic location, may be used as key words but will be followed by an indication of technical context. The assignment of links, rules, and weights is optional.

UNCLASSIFIED

Security Classification